Spectral observation of conversion between ionized *vs.* non-ionized proton-coupled electron transfer interfaces†

Elizabeth R. Young, Joel Rosenthal and Daniel G. Nocera

Received (in Austin, TX, USA) 15th November 2007, Accepted 29th February 2008
First published as an Advance Article on the web 14th April 2008
DOI: 10.1039/b717747j

Two-point hydrogen bonding between acid and base functionalities provides a convenient method for the modular assembly of proton-coupled electron transfer (PCET) networks, especially when that interface comprises an amidinium and two-point anionic partner; a system is presented that permits the proton configuration within the interface to be determined when pK_a values of the conjugate acids are known.

Proton-coupled electron transfer (PCET) may be established within donor–acceptor dyads assembled by a hydrogen bonded interface.[1,2] PCET networks assembled from Watson–Crick base pairs[3] and dicarboxylic acid dimers[4] do not support proton transfer within the interface thus limiting the extent to which PCET may be investigated. For this reason, the asymmetric proton interface of an amidinium bound to two-point, anionic partners, especially carboxylate, has come to the fore.[5–10] The two tautomers shown in Chart 1 are possible: an ionized amidinium–carboxylate or a non-ionized amidine–carboxylic acid, both of which can support proton transfer along a PCET coordinate.

The amidinium–carboxylate interface combines the dipole of an electrostatic ion pair interaction, a two-point hydrogen bond, and secondary electrostatic interactions to produce a highly stable proton interface.[11–15] These factors along with the relative pK_a values of amidinium and carboxylate, conspire to determine the extent to which the interface configuration is ionized.[16] The electrostatic interactions within the interface stabilize charge accumulation, leading in some cases to an ionized interface even when a simple ΔpK_a calculation predicts formation of a non-ionized interface in a solution of a given dielectric constant.[10] We now show the ΔpK_a value necessary to achieve the ionized *vs.* the non-ionized interface by stepping through a series of binding moieties (BMs) with different acidity constants. The transition from a non-ionized to ionized interface occurs as the acidity of the BM increases.

Efficient binding of an amidinium (amH^+) to carboxylate and sulfonate anions occurs in aprotic solvents of low dielectric constant. A series of BMs of varying pK_a values in ACN was chosen as summarized in Table 1.[17,18] The trend in the dependence of the amH^+:BM^- association and interface configuration on the dielectric constant of the solvent can be probed along

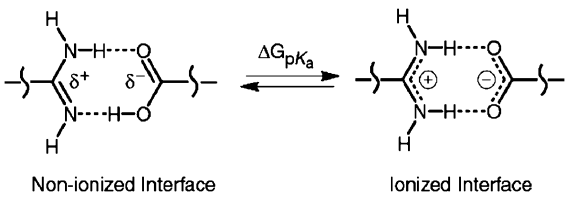

Chart 1

the series tetrahydrofuran (THF, $\varepsilon = 7.58$), dichloromethane (DCM, $\varepsilon = 8.93$) and acetonitrile (ACN, $\varepsilon = 37.5$).[19]

Interrogation of the proton configuration of the amidinium interface was accomplished using purpurin **1**, in which conjugation is maintained between the amidinium and porphyrin *via* an unsaturated five-membered ring. We have shown that the absorption spectrum of **1** is sensitive to its protonation state.[10] Reduction of the five-membered isocyclic ring of **1** yields the corresponding chlorin homologue. Unlike **1**, the absorption spectrum of the chlorin–amidinium is invariant with pH (see Fig. S1, ESI†).

Fig. 1 shows the absorption spectrum of **1** before (**1-amH$^+$**) and after (**1-am**) addition of the base 4-dimethylaminopyridine (DMAP). Deprotonation of the amidinium functionality in ACN is indicated by a shift in the absorption maximum of the Soret band from 428 to 423 nm (Fig. 1(c)). Similar spectral trends are observed in THF and DCM (Fig. 1(a) and (b), respectively). Absorption spectra (Fig. S2–S4, ESI†) demonstrate analogous spectral shifts with each BM and exhibit well-anchored isosbestic points during the titration of the BM with **1-amH$^+$**. A 1 : 1 binding motif is signified from a Benesi–Hildebrand analysis of the titration data ($1/\Delta A$ *vs.* 1/[BM]) (Fig. S2–S4, ESI†).[20] The binding constant, K_{assoc}, for **1**:**2** is found to be $\sim 4.5 \times 10^4$ M^{-1} and for **1**:**3** is $\sim 1.5 \times 10^2$ M^{-1} in ACN. The K_{assoc} for **4**, **5** and **6** are all the same within error and are measured to be $\sim 9.9 \times 10^3$ M^{-1}.

The endpoint spectrum of each titration reveals the configuration of the proton interface as indicated by the final

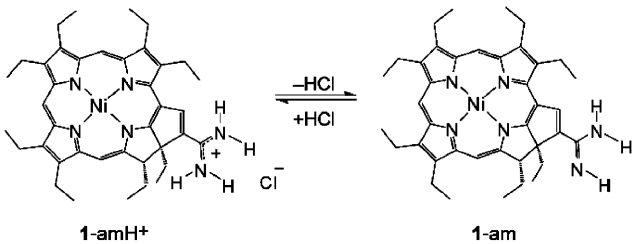

Scheme 1

Department of Chemistry, 6-335, Massachusetts Institute of Technology, 77 Massachusetts Ave., Cambridge, MA 02139-4307, USA. E-mail: nocera@mit.edu; Fax: 01 617 253 7670; Tel: 01 617 253 5537

† Electronic supplementary information (ESI) available: Experimental procedures, additional spectra and charts. See DOI: 10.1039/b717747j

Table 1 ΔG_{pK_a} and interface configuration for **1**:BM complexes

	Binding moiety	pK_a[a]	ΔG_{pK_a}/eV (**1**:BM)[b]	Ionized interface? THF	DCM	ACN
1	Purpurin-amH$^+$	9.55				
2	3,5-Dinitrobenzoate	17	0.44	✓	✓	✓
3	Phenylsulfonate	7	−0.15	✓	✓	✓
4	Acetate	21	0.68			
5	Chloroacetate	18	0.50		✓	
6	Dichloroacetate	14	0.26	✓	✓	✓

[a] In CH_3CN, from ref. 17. [b] At 298 K, calculated from pK_a values recorded in ACN, $\Delta G_{pK_a} = -RT[pK_a(BM)/pK_a(\mathbf{1}\text{-}\mathbf{am}^+)]$.

position of the Soret ($S_2 \leftarrow S_0$ transition at ~430 nm) or Q-band ($S_1 \leftarrow S_0$ transition at ~650 nm) maximum. Conversion of **1-amH**$^+$ to **1-am** in the non-ionized interface is indicated by a shift of the peak maxima to wavelengths nearly coincident with that observed for **1-am** upon deprotonation of **1-amH**$^+$ with DMAP. We interpret the small 1–2 nm shifts of the Soret band of **1-amH**$^+$ in the presence of the BM to the establishment of a non-ionized amidine–carboxylic acid interface.[10]

Fig. 1 (inset) shows the final Soret peak position of **1** in each solvent for all BMs studied. The solid data points at each end represent the peak position of **1-amH**$^+$ (highest wavelength) and **1-am** (lowest wavelength). The dotted line in each plot shows an approximate boundary for the transition between the ionized to non-ionized interface as determined by the final Soret position, and augmented by spectral analysis of the initial and final spectra (see ESI† for details of spectral analysis). The unavailability of additional BMs with precise pK_a values limits the observation of a clearly identifiable pK_a transition between the two tautomers.

Experimental observation of the proton interface configuration for each BM and determination of K_{assoc} for a given interface enables the construction of the thermodynamic cycle shown in Scheme 2. Since the interface under consideration is formed from amH$^+$ and ^-O_2C as the reactants (Scheme 2 top, left), either an amH$^+\cdots{}^-O_2C$ or an am$\cdots$HO$_2$C interface is produced. The driving force for formation of the former (ΔG_1) is measured directly from the measurement of K_{assoc} for the ionized **1-amH**$^+$:$^-$**O$_2$C** complex, while the driving force for the latter (ΔG_3) is determined for the non-ionized

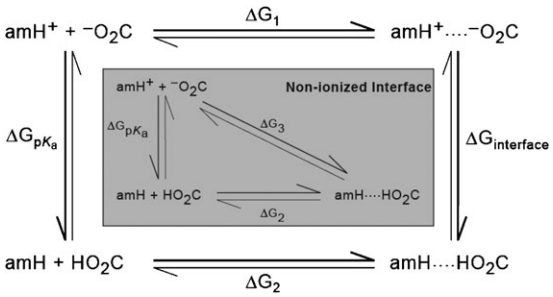

Scheme 2 Square scheme representation of free energies involved in determining the tautomeric form of the interface.

1-am$\cdots$**HO$_2$C** complex (Scheme 2, inset). The driving force for formation of am$\cdots$HO$_2$C from the neutral analogues (ΔG_2) can be determined by the difference between the ΔG_3 and ΔG_{pK_a} as shown by the inset in Scheme 2,

$$\Delta G_2 = \Delta G_3 - \Delta G_{pK_a} \quad (1)$$

Accordingly, the stabilization imparted by proton transfer within the interface ($\Delta G_{interface}$) can be determined from the free energies of the square scheme and the pK_as of the constituent moieties (ΔG_{pK_a}).

Although the binding of the various BMs of Table 1 to **1-amH**$^+$ was carried out in ACN, DCM and THF, the thermodynamic description and stabilization energy of the interface outlined above can only be rigorously determined for ACN since pK_a values for the BMs used in this study have been determined in this solvent. Inspection of Fig. 1(c) reveals that conversion between the tautomeric forms of the interface occurs between BMs **4** and **5**. Thus, Scheme 2 is analyzed for these two BMs as they most closely define the razor's edge between formation of the ionized and neutral hydrogen bonding interface. Accordingly, these two points allow for the determination of the minimum interface stabilization necessary to obtain an ionized interface as per eqn (2):

$$\Delta G_{interface} = (\Delta G_2 + \Delta G_{pK_a}) - \Delta G_1 \quad (2)$$

The am$\cdots$HO$_2$C tautomer is formed upon association of **1-amH**$^+$ with **4**, allowing for the determination of ΔG_2 *via* eqn (1). ΔG_1 is obtained from K_{assoc}(**1**:**5**), since association of **1-amH**$^+$ with **5** generates the ionized **amH**$^+$:$^-$**O$_2$C** complex.

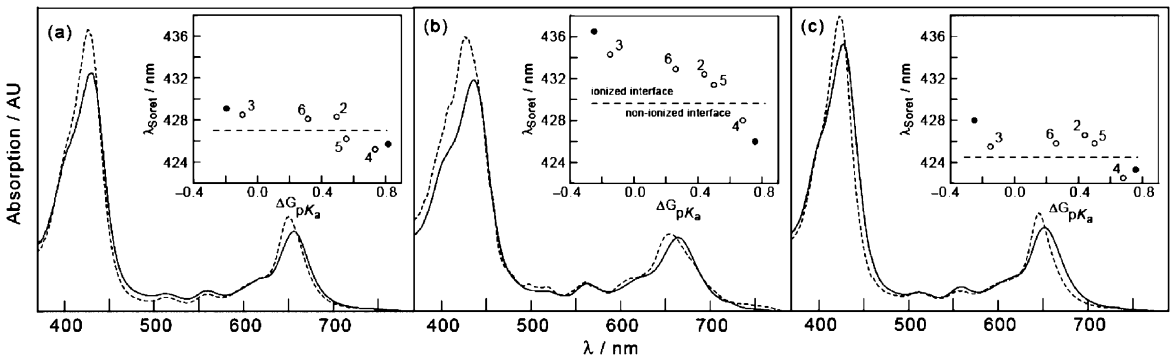

Fig. 1 UV-visible absorption spectra of **1-amH**$^+$, solid line; **1-am** formed by deprotonated of **1-amH**$^+$ with DMAP, dotted line. (a) λ_{max}(**1-amH**$^+$) = 430 nm shifts to λ_{max}(**1-am**) = 426 nm in THF, 2000 eq. DMAP, (b) λ_{max}(**1-amH**$^+$) = 436 nm shifts to λ_{max}(**1-am**) = 426 nm in DCM, 550 eq. DMAP and (c) λ_{max}(**1-amH**$^+$) = 428 nm shifts to λ_{max}(**1-am**) = 423 nm in ACN, 950 eq. DMAP. Inset: Soret peak position of the purpurin *vs.* ΔG_{pK_a} for each of the associated **1**:BM complexes. The highest and lowest peak maxima (solid circles) represent **1-amH**$^+$, solid line; **1-am**, respectively.

Table 2 Calculated free energy values for thermodynamic considerations for assignment of $\Delta G_{\text{Interface}}$ in ACN

Binding moiety (BM)		pK_a[a]	ΔG_1[b]/eV	ΔG_2/eV	ΔG_3/eV[b]	ΔG_{pK_a}[c]/eV	$\Delta G_{\text{interface}}$/eV
1	Purpurin-amH$^+$	9.55	—	—	—	—	—
2	3,5-Dinitrobenzoate	17	−0.28	—	—	−0.44	—
3	Phenylsulfonate	7	−0.13	—	—	0.15	—
4	**Acetate**	**21**	—	**0.44**	**−0.24**	**−0.68**	**0.18**
5	**Chloroacetate**	**18**	**−0.24**	—	—	**−0.50**	
6	Dichloroacetate	14	−0.24	—	—	−0.26	—

[a] In CH_3CN, from ref. 17. [b] $\Delta G = -RT\ln K_{\text{assoc}}$(**1**:**BM**). [c] At 298 K, calculated from pK_a values recorded in ACN, $\Delta G_{pK_a} = -RT[pK_a(\textbf{BM})/pK_a(\textbf{1-amH}^+)]$.

That the ionized interface for **1**:**5** persists when the pK_a difference dictates formation of the am$\cdots$$HO_2C$ interface reveals the importance of electrostatic contributions to the interface configuration. The electrostatic stabilization of the interface imparted by formation of the ionized **amH**$^+$:$^-$**O$_2$C** complex ($\Delta G_{\text{interface}}$) can be determined using eqn (2); it is minimally 0.18 eV in ACN. This electrostatic interaction energy can be calculated for point charges, q_1 and q_2, according to $V = (q_1q_2)/(4\pi\varepsilon r)$ where ε is the dielectric constant of the medium.[21] An electrostatic stabilization energy of 0.10 eV is calculated for the amidinium–carboxylate salt bridge at a distance of r = 3.9 Å in THF. This distance is measured between the central carbon atoms of the amidinium and carboxylate groups from the energy optimized structure.[8] The experimental results reported here agree with a simple ion solvation model. The discrepancy likely arises from the approximation that the electrostatic charge within the interface is confined to a point-dipole (Table 2).

While the dearth of known pK_a values in DCM and THF preclude a similar thermodynamic analysis in those solvents, a qualitative understanding of interface behaviour is inferred from experimental results. In the dielectric environment of DCM, the proton interface maintains the ionized configuration at the same ΔpK_a difference as ACN, however in the lower dielectric environment of THF conversion to the ionized tautomer shifts to lower ΔpK_a. THF does not tolerate charge build-up to the extent that ACN and DCM do, and thereby favours a non-ionized interface configuration at a lower free energy.

The energetics of the amidinium–carboxylate interface are essential to assigning a general interface stabilization energy with the goal of accurately projecting the tautomeric state of the proton interface to PCET systems. For example, the hydrogen bonded donor–acceptor, system D–[H$^+$]–A (D = amidinium appended Zn(II)TMP, A = naphthalene diimide carboxylic acid) reveals a PCET rate of 9.50×10^8 s^{-1} with a kinetic isotope effect (KIE) of 1.06 at room temperature.[9] In this case, the interface is the non-ionized amidine–carboxylic acid tautomer. When this D–[H$^+$]–A system is subtly altered to produce an ionized amidinium–sulfonate interface (A = naphthalene diimide sulfonic acid) of similar driving force, (Table 1, represented by the **1**:**3** interface), the change in interface configuration has a clear effect on the PCET rate and solvent dependent ET parameters ($|V|$, λ, E_{act}).[22] The PCET rate roughly doubles to 19×10^8 s^{-1} with a KIE of 1.17 and more strikingly ET parameters show a clear solvent dependence through the ionized interface, which is absent in the first system. The enhancement of PCET rate and solvent dependent ET parameters for the same D–A pair bearing different tautomeric forms of the interface, illustrates the pronounced effect that proton position exerts on photoinduced charge transfer.

Notes and references

1 C. J. Chang, J. D. Brown, M. C. Y. Chang, E. A. Baker and D. G. Nocera, in *Electron Transfer in Chemistry*, ed. V. Balzani, Wiley-VCH, Weinheim, Germany, 2001, vol. 3.2.4, pp. 409–461.
2 R. I. Cukier and D. G. Nocera, *Annu. Rev. Phys. Chem.*, 1998, **49**, 337–369.
3 J. L. Sessler, B. Wang, S. L. Springs and C. T. Brown, in *Comprehensive Supramolecular Chemistry*, ed. Y. Murakami, Pergamon Press, Oxford, 1996, vol. 4, pp. 311–336, and references therein.
4 C. Turró, C. K. Chang, G. E. Leroi, R. I. Cukier and D. G. Nocera, *J. Am. Chem. Soc.*, 1992, **114**, 4013–4015.
5 J. A. Roberts, J. P. Kirby and D. G. Nocera, *J. Am. Chem. Soc.*, 1995, **117**, 8051–8052.
6 J. A. Roberts, J. P. Kirby, S. T. Wall and D. G. Nocera, *Inorg. Chim. Acta*, 1997, **263**, 395–405.
7 J. A. Roberts, J. P. Kirby and D. G. Nocera, *J. Am. Chem. Soc.*, 1997, **119**, 9230–9236.
8 N. H. Damrauer, J. M. Hodgkiss, J. Rosenthal and D. G. Nocera, *J. Phys. Chem. B*, 2004, **108**, 6315–6321.
9 J. M. Hodgkiss, N. H. Damrauer, S. Presse, J. Rosenthal and D. G. Nocera, *J. Phys. Chem. B*, 2006, **110**, 18853–8.
10 J. Rosenthal, J. M. Hodgkiss, E. R. Young and D. G. Nocera, *J. Am. Chem. Soc.*, 2006, **128**, 10474–10483.
11 J. Pranata, S. G. Wierschke and W. L. Jorgensen, *J. Am. Chem. Soc.*, 1991, **113**, 2810–2819.
12 T. Uchimaru, J. Korchowiec, S. Tsuzuki, K. Matsumura and S. Kawahara, *Chem. Phys. Lett.*, 2000, **318**, 203–209.
13 O. Lukin and J. Leszczynski, *J. Phys. Chem. A*, 2002, **106**, 6775–6782.
14 O. Lukin and J. Leszczynski, *J. Phys. Chem. A*, 2003, **107**, 9251–9252.
15 S. Schlund, C. Schmuck and B. Engels, *J. Am. Chem. Soc.*, 2005, **127**, 11115–11124.
16 J. M. Hodgkiss, J. Rosenthal and D. G. Nocera, in *Handbook of Hydrogen Transfer. Physical and Chemical Aspects of Hydrogen Transfer*, ed. J. T. Hynes, J. P. Klinman, H.-H. Limbach and R. L. Schowen, Wiley-VCH, Weinheim, Germany, 2006, vol. 2.4.17, pp. 503–562.
17 K. Izutsu, *Acid–Base Dissociation Constants in Dipolar Aprotic Solvents*, Blackwell Scientific, Cambridge, USA, 1990.
18 The pK_a range reported for each BM are as follows: acetate (**4**) pK_a = 20–22; chloroacetate (**5**) pK_a = 15–19; and, dichloroacetate (**6**) pK_a = 13–15. The pK_a of phenylsulfonate (**3**) is estimated to be 8 from vales for *p*-toluenesulfonic acid, pK_a = 8 and 2.5-dichlorobenzenesulfonic acid, pK_a = 6.2–6.4.
19 Y. Marcus, in *Ion Solvation*, Wiley, Chichester, 1985, pp. 136–137.
20 K. A. Connors, in *Binding Constants: A Measurement of Molecular Complex Stability*, Wiley, New York, 1987.
21 Y. Marcus, in *Ion Solvation*, John Wiley, Chichester, 1985, p. 136.
22 E. R. Young, J. R. Rosenthal, J. M. Hodgkiss and D. G. Nocera, manuscript in preparation.

